Supporting Information:

Morphology and hygroscopicity of nanoplastics in sea spray

Sarah Suda Petters,[a,†] Eva Rosendal Kjærgaard,[a] Freja Hasager,[a] Andreas Massling,[b] Marianne Glasius,[a] Merete Bilde[a]

[a] Department of Chemistry, Aarhus University, Langelandsgade 140, 8000 Aarhus C, Denmark. Merete Bilde <bilde@chem.au.dk>
[b] Department of Environmental Science, Aarhus University, Frederiksborgvej 399, 4000 Roskilde, Denmark.
† Present address: Bourns College of Engineering Center for Environmental Research and Technology, University of California Riverside, 1084 Columbia Ave, Riverside, CA 92507. Sarah Suda Petters <sarah.petters@ucr.edu>

Contents

Section S1. Experiment List

Table S1 (over the next pages) details the experiments performed.

Table S1. Experiment list. Experiment numbers (**Exp #**) are referenced in the captions of Figure 3, Figure 4, and Figure 7. Solution numbers (**Soln #**) identify the aerosolized mixture (Table 1 of the main text). Three configurations of the instrument described in the main text are reported in the **Type** column: HTDMA, SEMS, and HTDMA-AMS. Dry diameter (**D_{dry}**) is scanned in SEMS mode and held constant in HTDMA and HTDMA-AMS modes. **Wet RH** refers to the relative humidity in the HTDMA (DMA 2 in Figure 1). The number of seconds per bin (**s/bin**) and the number of bins (**Bins**) are multiplied together to give the total scan time (**Scan**) in either the SEMS or the HTDMA instrument. **c_{tot}** is the total number concentration reported by the SEMS or HTDMA instrument software, and **m_{tot}** is the total mass concentration reported by the SEMS software. Table S10 shows the results of growth factor inversion calculations for select experiments listed here.

Exp # -	**Soln #** -	**Salinity** g kg^{-1}	**PSL** mg kg^{-1}	**Type** -	D_{dry} nm	**DMA 1** Q_{sh} / Q_{sa} L min^{-1}	**Dry RH** %	D_{wet} nm	**DMA 2** Q_{sh} / Q_{sa} L min^{-1}	**Wet RH** %	**Date** mmm	**Date** dd(#)	**Time** hh:mm	**s/bin** s	**Bins** -	**Scan** s	c_{tot} cm^{-3}	m_{tot} µg m^{-3}
1	MilliQ	0	0	HTDMA	150	5.00 / 0.965	3.7	75-500	5.00 / 0.508	75	Feb	11a	11:51-12:14	1	60	60	5.8	
2	8	0	0.18	HTDMA	150	5.00 / 0.977	3.9	75-500	5.00 / 0.509	75	Feb	11b	12:18-12:41	2	60	120	219.2	
3	7	7.52e-5	0.18	HTDMA	150	5.00 / 0.979	3.9	75-500	5.01 / 0.507	75	Feb	11c	12:51-13:30	2	60	120	242.6	
4	6	4.96e-4	0.18	HTDMA	150	5.00 / 0.992	4	75-500	5.00 / 0.514	74.9	Feb	11d	13:32-13:53	2	60	120	296.2	
5	6	4.96e-4	0.18	SEMS	5-600	5.00 / 0.992	4.2				Feb	11-s1	14:00-14:06	1	60	60	163505	2.8
6	5	3.27e-3	0.18	SEMS	5-1000	5.00 / 1.000	4				Feb	11-s2	14:08-14:11	3	60	180	387555	28.2
7	5	3.27e-3	0.18	SEMS	5-1000	3.00 / 0.596	3.7				Feb	11-s3	14:19-14:30	3	60	180	290553	11.4
8	5	3.27e-3	0.18	HTDMA	150	5.00 / 1.016	4	75-500	5.00 / 0.521	74.9	Feb	11e	14:31-14:33	2	60	120	370	
9	4	0.022	0.18	HTDMA	150	5.00 / 1.002	4.2	75-500	5.00 / 0.522	75	Feb	11f	14:36-14:50	2	60	120	511.3	
10	4	0.022	0.18	SEMS	5-1000	3.00 / 0.597	3.8				Feb	11-s4	14:53-15:00	3	60	180	878619	39
11	3	0.14	0.18	HTDMA	150	5.00 / 1.010	4.2	75-500	5.00 / 0.523	75	Feb	11g	15:04-15:11	2	60	120	9170.4	
12	3	0.14	0.18	SEMS	5-1000	3.00 / 0.592	3.8				Feb	11-s5	15:13-15:20	3	60	180	2193940	238.5
13	2	0.94	0.18	SEMS	5-1000	3.00 / 0.599	3.6				Feb	11-s6	15:25-15:32	3	60	180	3845974	1474
14	2	0.94	0.18	HTDMA	150	5.00 / 1.006	4.4	75-500	5.00 / 0.514	74.9	Feb	11h	15:33-15:40	2	60	120	87195.2	
15	1	6.21	0.18	HTDMA	150	5.00 / 1.007	4.4	75-500	5.00 / 0.514	74.8	Feb	11i	15:44-15:49	2	60	120	383259	
16	1	6.21	0.18	SEMS	5-1000	3.00 / 0.591	3.9				Feb	11-s7	15:50-15:53	3	60	180	4886690	8219.9
17	MilliQ	0	0	SEMS	5-1000	3.00 / 0.577	2.7				Feb	14-s1	11:08-11:18	3	60	180	64434	4
18	MilliQ	0	0	HTDMA	150	5.00 / 0.913	3.8	75-500	5.00 / 0.520	75.2	Feb	14a	11:30-11:34	2	60	120	3.1	
19	8	0	0.18	HTDMA	150	5.00 / 0.934	3.8	75-500	5.00 / 0.520	74.9	Feb	14b	11:38-11:45	2	60	120	261.6	

Exp # -	**Soln #** -	**Salinity** g kg^{-1}	**PSL** mg kg^{-1}	**Type** -	D_{dry} nm	**DMA 1** Q_{sh} / Q_{sa} L min^{-1}	**Dry RH** %	D_{wet} nm	**DMA 2** Q_{sh} / Q_{sa} L min^{-1}	**Wet RH** %	**Date** mmm	**Date** dd(#)	**Time** hh:mm	**s/bin** s	**Bins** -	**Scan** s	c_{tot} cm^{-3}	m_{tot} µg m^{-3}
20	8	0	0.18	SEMS	5-1000	3.00 / 0.562	3.3				Feb	14-s2	11:47-11:51	2	60	120	93338	6.3
21	7	7.52e-5	0.18	SEMS	5-1000	3.00 / 0.570	3.1				Feb	14-s3	11:53-11:58	2	60	120	119702	6.9
22	7	7.52e-5	0.18	HTDMA	150	5.00 / 0.956	3.8	75-500	5.00 / 0.512	74.9	Feb	14c	12:05-12:12	2	60	120	323.8	
23	6	4.96e-4	0.18	HTDMA	150	5.00 / 0.961	3.9	75-500	5.00 / 0.510	74.5	Feb	14d	12:14-12:18	2	60	120	330.3	
24	6	4.96e-4	0.18	SEMS	5-1000	3.00 / 0.569	3.4				Feb	14-s4	12:20-12:25	2	60	120	145373	7
25	5	3.27e-3	0.18	SEMS	5-1000	3.00 / 0.577	3.2				Feb	14-s5	12:28-12:33	2	60	120	298303	12.4
26	5	3.27e-3	0.18	HTDMA	150	5.00 / 0.935	4.2	75-500	5.02 / 0.491	76.4	Feb	14e	12:40-12:44	2	60	120	345.3	
27	4	0.022	0.18	HTDMA	150	5.00 / 0.971	4.2	75-500	4.99 / 0.524	75	Feb	14f	12:48-12:52	2	60	120	481.8	
28	4	0.022	0.18	SEMS	5-1000	3.00 / 0.572	3.6				Feb	14-s6	12:54-12:58	2	60	120	838115	41.3
29	3	0.14	0.18	SEMS	5-1000	3.00 / 0.577	3.3				Feb	14-s7	13:03-13:08	2	60	120	2076754	238.9
30	3	0.14	0.18	HTDMA	150	5.00 / 0.960	3.7	75-500	5.01 / 0.506	75	Feb	14g	13:09-13:14	2	60	120	8675.2	
31	2	0.94	0.18	HTDMA	150	5.00 / 0.972	4	75-500	5.00 / 0.520	75	Feb	14h	13:17-13:24	2	60	120	85012	
32	2	0.94	0.18	SEMS	5-1000	3.00 / 0.572	3.6				Feb	14-s8	13:26-13:30	2	60	120	3710872	1566
33	1	6.21	0.18	SEMS	5-1000	3.00 / 0.573	3.3				Feb	14-s9	13:33-13:38	2	60	120	4837814	9774
34	1	6.21	0.18	HTDMA	150	5.00 / 0.971	3.8	75-500	5.00 / 0.517	75	Feb	14i	13:39-13:46	2	60	120	389662	
35	A+PSL	41	0.18	SEMS	5-1000	3.00 / 0.560	5.7				Feb	14-s10	14:09-14:13	2	60	120	5335758	42617
36	A+PSL	41	0.18	HTDMA	150	5.01 / 0.835	6.4	75-500	5.00 / 0.472	75	Feb	14k	14:35-14:39	2	60	120	575486.2	
37	A+PSL	41	0.18	SEMS	5-1000	3.00 / 0.556	4.7				Feb	14-s11	14:42-14:46	2	60	120	5208632	47544.6
38	room air			SEMS	5-1000	3.00 / 0.571	4.4				Feb	14-s14	15:38-15:42	2	60	120	471.6	0.7
39	room air			HTDMA	150	5.00 / 0.797	3.3	75-500	5.00 / 0.322	75	Mar	02a	13:37-13:46	2	60	120	0.3	
40	MilliQ	0	0	HTDMA	150	5.00 / 0.983	3.9	75-500	5.00 / 0.518	75.1	Mar	02b	13:48-14:06	2	60	120	8.3	
41	MilliQ	0	0	SEMS	5-1000	3.00 / 0.576	3.5				Mar	02-s1	14:11-14:14	3	60	180	37131.8	2.9
42	2d	0.151	0.18	SEMS	5-1000	3.00 / 0.584	3.4				Mar	02-s2	14:18-14:28	3	60	180	1740916	223.4
43	2d	0.151	0.18	HTDMA	150	5.00 / 0.974	4	75-500	5.00 / 0.506	75.1	Mar	02c	14:42-14:46	2	60	120	9350.1	
44	2c	0.239	0.18	HTDMA	150	5.00 / 0.977	4	75-500	5.00 / 0.509	75	Mar	02d	15:07-15:14	2	60	120	14309.5	
45	2c	0.239	0.18	SEMS	5-1000	3.00 / 0.575	3.5				Mar	02-s3	15:27-15:33	3	60	180	2248376	393
46	2b	0.378	0.18	SEMS	5-1000	3.00 / 0.579	3.4				Mar	02-s4	15:36-15:42	3	60	180	2443773	510.8
47	2b	0.378	0.18	HTDMA	150	5.00 / 0.970	3.8	75-500	5.00 / 0.508	74.9	Mar	02f	15:46-15:50	2	60	120	22258.2	
48	2a	0.596	0.18	HTDMA	150	5.00 / 0.970	4.1	75-500	5.00 / 0.508	74.9	Mar	02i	16:07-16:11	2	60	120	45109.3	
49	2a	0.596	0.18	SEMS	5-1000	3.00 / 0.825	4.7				Mar	02-s5	16:12-16:19	3	60	180	3007183	922.8
50	2d no PSL	0.151	0	HTDMA	150	6.50 / 1.013	3.1	10-1036	5.00 / 0.515	75	Apr	26a	10:56-12:56	24	300	7200	1255	
51	2d	0.151	0.18	HTDMA	150	6.50 / 1.015	3.1	10-1034	5.00 / 0.520	74.9	Apr	26b	13:09-13:16	2	60	120	3901	
52	2d	0.151	0.18	SEMS	10-827	6.50 / 0.659	2.2				Apr	26-s1	13:17-13:24	2	60	120	883110	82

Exp # -	**Soln #** -	**Salinity** g kg^{-1}	**PSL** mg kg^{-1}	**Type** -	D_{dry} nm	**DMA 1** Q_{sh} / Q_{sa} L min^{-1}	**Dry RH** %	D_{wet} nm	**DMA 2** Q_{sh} / Q_{sa} L min^{-1}	**Wet RH** %	**Date** mmm	**Date** dd(#)	**Time** hh:mm	**s/bin** s	**Bins** -	**Scan** s	c_{tot} cm^{-3}	m_{tot} µg m^{-3}
53	2d	0.151	0.18	HTDMA-AMS	150	6.50 / 0.975	2.9	10-1000	5.00 / 0.499	75	Apr	26c	14:07-15:42	19	300	5700		
54	2d	0.151	0.18	HTDMA-AMS	150	6.50 / 0.983	3.3	50-750	5.00 / 0.500	75	Apr	26d	15:51-17:57	25	300	7500		
55	MilliQ	0	0	HTDMA	150	6.50 / 0.969	3.2	10-1033	5.00 / 0.485	74.9	Apr	28a	09:36-10:01	5	300	1500	3.6	
56	MilliQ	0	0	SEMS	5-827	6.50 / 0.657	2.4				Apr	28-s1	10:15-10:20	2	60	120	13963	0.1
57	2c	0.239	0.18	SEMS	5-827	6.50 / 0.652	2.3				Apr	28-s2	10:37-10:41	2	60	120	1259805	183
58	2c	0.239	0.18	HTDMA	150	6.50 / 0.988	3	10-1032	5.00 / 0.499	75	Apr	28b	10:43-10:48	2	60	120	6280.4	
59	2c	0.239	0.18	HTDMA-AMS	150	6.50 / 0.981	3.3	10-1033	5.00 / 0.500	75	Apr	28c	10:50-12:55	25	300	7500		
60	2b	0.378	0.18	SEMS	5-827	6.50 / 0.654	2.4				Apr	28-s3	13:06-13:08	2	60	120	1959978	372.6
61	2b	0.378	0.18	SEMS	5-827	6.50 / 0.654	2.4				Apr	28-s3	13:06-13:08	2	60	120	1959978	372.6
62	2b	0.378	0.18	HTDMA	150	6.51 / 0.979	3	10-1032	5.00 / 0.502	75	Apr	28d	13:17-13:22	2	60	120	14959	
63	2b	0.378	0.18	HTDMA-AMS	150	6.50 / 0.989	3.4	25-1033	5.00 / 0.498	75	Apr	28e	13:23-15:28	25	300	7500		
64	2a	0.596	0.18	SEMS	5-827	6.50 / 0.658	2.4				Apr	28-s4	15:34-15:39	2	60	120	2062373	528.2
65	2a	0.596	0.18	HTDMA	150	6.51 / 0.977	3.1	25-1032	5.00 / 0.487	74.9	Apr	28f	15:40-15:44	2	60	120	22787	
66	2a	0.596	0.18	HTDMA-AMS	150	6.50 / 0.981	3.5	25-1033	5.00 / 0.485	75	Apr	28g	15:45-17:51	25	300	7500	1482298	
67	Ægor 1	0	0.15	SEMS	50-500	6.50 / 0.585	2.7				May	23-s1	13:13-13:20	2	60	120	26	0.1
68	Ægor 1	0	0.15	SEMS	50-500	5.00 / 0.536	3.3				May	23-s2	13:21-13:25	2	60	120	21.7	0.1
69	Ægor 1	0	0.15	HTDMA	150	5.37 / 0.884	4.6	100-300	4.99 / 0.496	74.9	May	23c	14:01-14:20	1	120	120	6.1	
70	Ægor 1	0	0.15	HTDMA-AMS	150	5.00 / 0.853	5	100-400	5.00 / 0.492	75	May	23d	14:27-16:32	25	300	7500		
71	Ægor 1	0	0.15	HTDMA	150	5.00 / 0.857	5.1	100-400	5.00 / 0.489	75.1	May	23e	16:36-16:43	1	180	180	36	
72	Ægor 2	0.01	0.15	SEMS	5-1039	5.00 / 0.534	4				May	23-s3	16:45-16:50	1	120	120	8000	1571.4
73	Ægor 2	0.01	0.15	SEMS	50-500	5.00 / 0.534	3.9				May	23-s4	16:51-16:55	1	120	120	62.2	0.2
74	Ægor 2	0.01	0.15	HTDMA	150	4.97 / 0.855	4.9	100-400	4.97 / 0.483	74.7	May	23f	16:57-17:01	1	180	180	36.6	
75	Ægor 2	0.01	0.15	HTDMA-AMS	150	5.00 / 0.859	5.5	100-400	5.00 / 0.503	75	May	23g	17:02-19:08	25	300	7500		
76	Ægor 2	0.01	0.15	HTDMA	150	5.00 / 0.879	5.5	100-400	5.00 / 0.504	74.9	May	23h	19:10-19:16	1	180	180	30.6	
77	Ægor 2	0.01	0.15	SEMS	50-500	5.00 / 0.534	4.2				May	23-s5	19:18-19:25	1	180	180	80.9	0.4
78	Ægor 2	0.01	0.15	SEMS	5-1040	5.00 / 0.530	4.1				May	23-s6	19:26-19:29	1	180	180	6556	718.9
79	Ægor 3	0.0215	0.15	SEMS	5-1038	5.00 / 0.554	4.6				May	24-s1	10:03-10:10	1	180	180	11760	98.5
80	Ægor 3	0.0215	0.15	HTDMA	150	5.00 / 0.852	5	100-400	5.00 / 0.499	75	May	24a	10:25-10:48	1	180	180	29.4	
81	Ægor 3	0.0215	0.15	HTDMA-AMS	150	5.00 / 0.845	4.8	100-400	5.00 / 0.513	75	May	24b	10:51-12:57	25	300	7500		
82	Ægor 4	0.0464	0.15	SEMS	5-1036	5.00 / 0.516	3.8				May	24-s2	13:07-13:14	1	180	180	16164	391.6
83	Ægor 4	0.0464	0.15	HTDMA	150	5.00 / 0.836	5	100-400	5.00 / 0.502	75.1	May	24c	13:23-13:27	1	180	180	41.2	
84	Ægor 4	0.0464	0.15	HTDMA	150	3.00 / 0.817	6.1	100-400	5.00 / 0.519	75	May	24d	13:28-13:34	1	180	180	43.3	
85	Ægor 4	0.0464	0.15	HTDMA-AMS	150	3.00 / 0.797	6.4	100-400	5.00 / 0.501	75	May	24e	13:37-15:43	25	300	7500		

Exp # -	**Soln #** -	**Salinity** g kg^{-1}	**PSL** mg kg^{-1}	**Type** -	D_{dry} nm	**DMA 1** Q_{sh} / Q_{sa} L min^{-1}	**Dry RH** %	D_{wet} nm	**DMA 2** Q_{sh} / Q_{sa} L min^{-1}	**Wet RH** %	**Date** mmm	**Date** dd(#)	**Time** hh:mm	**s/bin** s	**Bins** -	**Scan** s	c_{tot} cm^{-3}	m_{tot} µg m^{-3}
86	Ægor 5	0.1	0.15	HTDMA	150	3.00 / 0.789	6.9	100-400	5.00 / 0.503	74.9	May	24f	15:48-16:08	1	180	180	42.4	
87	Ægor 5	0.1	0.15	SEMS	5-1500	3.00 / 0.480	5.7				May	24-s3	16:13-16:19	1	180	180	25800	2.6
88	Ægor 5	0.1	0.15	SEMS	100-400	3.00 / 0.481	5.5				May	24-s4	16:20-16:27	1	180	180		
89	Ægor 5	0.1	0.15	HTDMA-AMS	150	3.00 / 0.791	7.7	100-400	5.00 / 0.497	75	May	24g	16:30-18:35	25	300	7500		
90	Ægor 6	0.2154	0.15	SEMS	5-1649	3.00 / 0.504	5.6			1	May	25-s1	10:26-10:33	1	180	180	53782	1.9
91	Ægor 6	0.2154	0.15	HTDMA	150	3.00 / 0.790	6.6	5-1034	5.00 / 0.486	75	May	25a	10:35-10:59	1	180	180	26.2	
92	Ægor 6	0.2154	0.15	HTDMA	150	3.00 / 0.810	6.6	100-400	5.00 / 0.492	74.9	May	25b	10:59-11:12	1	180	180	63.5	
93	Ægor 6	0.2154	0.15	HTDMA-AMS	150	3.00 / 0.815	6.7	100-400	5.00 / 0.505	75	May	25c	11:32-13:37	25	300	7500		
94	Ægor 7	0.464	0.15	SEMS	5-1645	3.00 / 0.488	5			1	May	25-s2	13:47-13:54	1	180	180		
95	Ægor 7	0.464	0.15	HTDMA	150	3.00 / 0.810	6.5	5-1034	5.00 / 0.496	74.9	May	25d	14:01-14:08	1	180	180	84.8	
96	Ægor 7	0.464	0.15	HTDMA	150	3.00 / 0.808	6.6	100-400	5.00 / 0.497	75	May	25e	14:09-14:19	1	180	180	240	
97	Ægor 7	0.464	0.15	HTDMA-AMS	150	3.00 / 0.820	7	100-400	5.00 / 0.512	75	May	25f	14:21-16:26	25	300	7500		
98	Ægor 7	0.464	0.15	HTDMA	150	3.00 / 0.804	6.9	100-400	5.00 / 0.495	75.2	May	25g	16:34-16:51	1	300	300		
99	Ægor 8	1	0.15	HTDMA	150	3.00 / 0.793	6.8	100-400	5.00 / 0.488	74.9	May	25h	16:56-17:01	1	300	300	1328	
100	Ægor 8	1	0.15	SEMS	5-1645	3.00 / 0.486	5.2			1	May	25-s3	17:03-17:15	1	180	180		
101	Ægor 8	1	0.15	HTDMA	150	3.00 / 0.784	6.4	100-400	5.00 / 0.485	75	May	25i	17:18-17:20	1	120	120	372	
102	Ægor 8	1	0.15	HTDMA-AMS	150	3.00 / 0.804	7	100-400	5.00 / 0.496	75	May	25j	17:22-19:52	30	300	9000		
103	Ægor 8	1	0.15	HTDMA	150	3.00 / 0.810	7	100-400	5.00 / 0.497	74.9	May	25k	20:21-20:25	1	120	120	312	
104	Ægor 8	1	0.15	SEMS	5-1645	3.00 / 0.488	5			1	May	25-s4	20:27-20:32	1	180	10		
105	no	0	0	SEMS	5-1035	5.00 / 0.535	3.7			1	Jun	02-s1	11:36-12:56	180	180	180	60.4	30.9
106	Ægor 9	0	0	SEMS	5-1033	5.00 / 0.525	3.3			1	Jun	02-s2	12:57-13:27	180	180	180	134.8	36.1
107	Ægor 9	0	0	HTDMA	150	5.00 / 0.829	4.5	100-400	5.00 / 0.488	75.1	Jun	02a	13:34-14:14	0.33	180	60	0.3	

Section S2. Instrumentation

S2.1. AMS Mass Resolution

Table S2 shows the mass resolution of the HR-ToF-AMS for selected experiments. The resolution was determined at calibration and remained close to the nominal value of 2500. The resolution indicates the number of bins relative to the m/z axis. Note that the ability to distinguish between ions with very similar masses is determined by the peak width, rather than the mass resolution.

Table S2. Mass resolution. The overall average resolution was $m/\Delta m$ = 2553 ±147.

Date 2022	Resolution, m/Δm	±1 std dev	Date 2022, cont'd	Resolution, m/Δm, cont'd	±1 std dev, cont'd
1-Mar	2653	140	26-Apr	2428	143
3-Mar	2645	139	28-Apr	2438	141
4-Mar	2636	127	2-May	2411	154
8-Mar	2587	161	4-May	2614	144
11-Mar	2578	118	9-May	2639	172
14-Mar	2459	164	11-May	2628	151
15-Mar	2516	166	23-May	2569	96
16-Mar	2560	143	24-May	2527	139
17-Mar	2527	175	25-May	2535	144
18-Mar	2561	177			

S2.2. AMS Vaporizer Characterization

Table S3 gives the measurements for this work that are shown in Figure 2.

Table S3. Vaporizer characterization. (A) Characterization of vaporizer control box setting "95", Figure 2, panel A, blue x's. (B) Ramping vaporizer setting, Figure 2, panel A, black crosses. (C) Vaporizer setting "80", Figure 2, panel A, blue x's. (D) Characterization of vaporizer temperature, Figure 2, panel C, black circles.

(A) Setting = 95

Current Amp	Voltage Volt	Power Watt	Date in 3/2022
1.20	4.84	5.82	14
1.21	4.86	5.80	14
1.17	4.87	5.81	14
1.21	4.82	5.71	15
1.18	4.86	5.79	15
1.20	4.86	5.84	17
1.18	4.86	5.75	17
1.21	4.86	5.80	17
1.18	4.87	5.71	17
1.20	4.87	5.71	17
1.19	4.88	5.86	18
1.18	4.87	5.76	18
Avg: 1.19	4.86	5.78	
Std Dev: 0.01	0.02	0.05	
R_{95}:	4.08 Ohm		

(B) Setting vs Current

Setting	Current Amp	Date in 3/2022
73	0.8	8
76	0.86	8
82	0.99	8
87	1.05	8
90	1.09	8
93	1.16	8
96	1.2	8
99	1.27	8
100	1.3	8
97	1.24	8
90	1.1	8
87	1.07	8

Table S3, cont'd.

(C) Setting = 80

	Current Amp	**Voltage** Volt	**Power** Watt	**Date in 3/2022**
	0.93	3.07	2.86	1
	0.93	3.07	2.86	1
	0.93	3.10	2.97	4
	0.95	3.08	2.93	14
	0.95	3.08	2.92	15
	0.93	3.11	2.92	18
Avg:	0.94	3.09	2.91	
Std Dev:	0.01	0.02	0.04	
R_{80}**:**		3.29 Ohm		

(D) Setting vs Temperature

Setting	**Current** Amp	**Power** Watt	**Temp** °C	**Tau** [a]	**Date in 3/2020**
73	0.8	1.9	465		10
78	0.9	2.5	500		10
83	1	3.27	532		10
89	1.1	4.38	571		10
95	1.2	5.7	812		10
73	0.8	1.9	430		10
78	0.9	2.55	532		10
81	0.95	3	580		10
83	1	3.3	570		10
86	1.04	3.9	610		10
89	1.09	4.4	648		10
92	1.13	5.1	560		10
95	1.19	5.8	682		10
98	1.24	6.2	808		10
73	0.8	1.9	440	0.00281	10
78	0.9	2.55	520	0.00039	10
81	0.95	3.05	606	0.00016	10
83	0.99	3.35	608	0.00012	10
86	1.04	3.9	629	9.93E-05	10
89	1.09	4.45	730	0.00011	10
92	1.13	5.15	800	9.09E-05	10
95	1.19	5.75	840	8.33E-05	10
98	1.24	6.2	822	8.26E-05	10

[a] Tau (in seconds) is for the m/z 30 signal from atomized NaNO3 measured by the AMS in PToF mode. See e.g. Williams et al. (2010).

S2.3. HTDMA Inversion

Figures S1 shows the results of the inversion used to find the hygroscopic growth factors from the humidified size distributions.

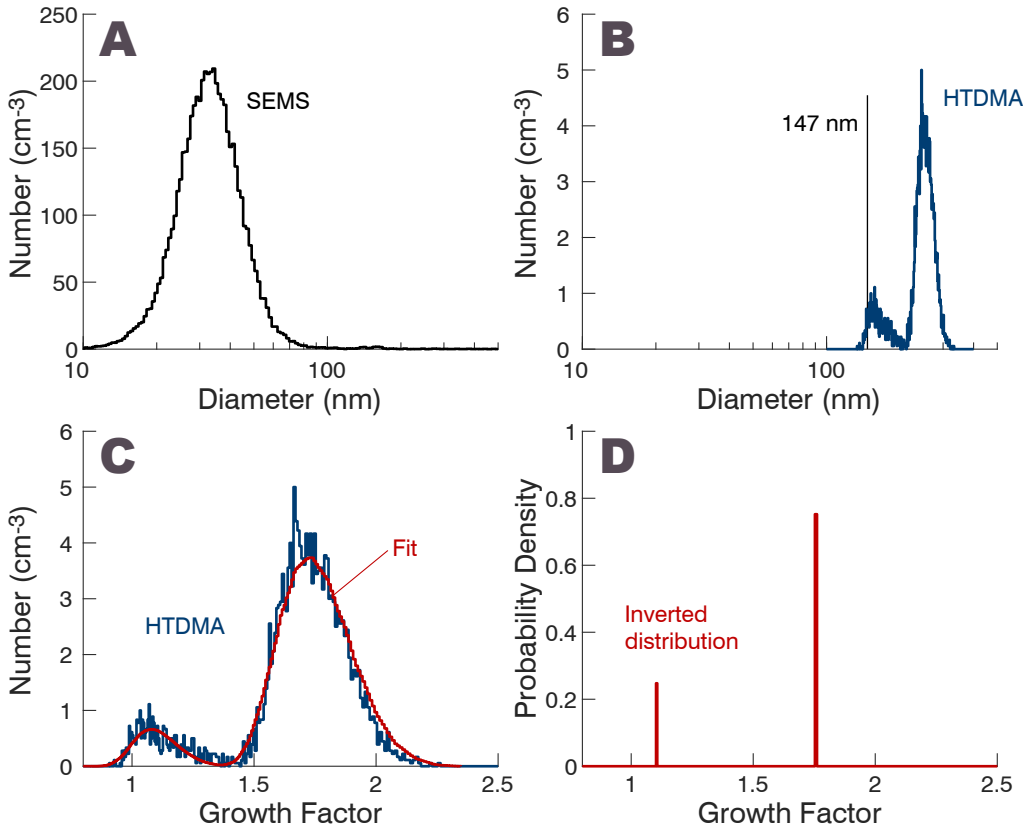

Figure S1. Growth factor inversion using RegularizationTools.jl (Petters, 2021), published under the GNU General Public License (https://github.com/mdpetters/RegularizationTools.jl). (A) Raw particle counts (experiment #94 in Table S1), (B) raw growth factor scan (experiment #98 in Table S1), (C) fitted two-component model, (D) inversion of fitted size distribution to approximate the distribution of particles between two growth factors (Fitted the growth factors were GF = 1.10 and GF = 1.76. Probability density is the fraction of particles falling into each growth factor bin. Note that the size distributions are not inverted and have units of particles per cm^3.

Section S3. AMS data analysis

The ToF-AMS Analysis Toolkit 1.65C (Squirrel 1.65C) was used to convert the time-of-flight signal to masses, apply the airbeam correction, and subtract the average background from each high-resolution mass spectrum. ToF-AMS HR Analysis 1.25C (Pika 1.25C) was used to determine the peak shape factor and prepare the background-subtracted, airbeam-corrected data for high-resolution analysis. MATLAB R2021a was used to convert peaks in the high-resolution spectra to ion signal (Hz) and to estimate the mass of species of interest ($\mu g\ m^{-3}$).

S3.1. Mass calibration

Data were loaded using ToF-AMS Analysis Toolkit 1.65C (Squirrel 1.65C; Sueper et al., 2011) and the m/z axis was calibrated using the ions listed in Table S4. The mass calibration

was performed independently for the open and closed mass spectra series to correct misalignment of peaks in the open and closed spectra. Equation S1.1 is used to match the ion's mass to its flight time:

$$x_{ToF} = p_1(t) + p_2(t)\, x_{mass}{}^{p_3(t)}. \qquad \text{Eq. S1}$$

Here, x_{mass} is the m/z value, x_{ToF} is the time-of-flight bin number, or, as identified in the SQUIRREL software, the sample number. Initial defaults of p_1 = -7215.10, p_2 = 2827.21, and p_3 = 0.5000 are used to find the peaks before correcting the mass axis. In this work, typical fitted values were p_1 = -7214, p_2 = 2827, and p_3 = 0.5. The typical resolution $m/\Delta m$ was ~2500.

Table S4. m/z calibration.

Ion	m/z	Used in this work?	Used by default in Squirrel 1.65C?
C+	12	yes, added	no
OH+	17.002739	yes	yes
H_2O+	18.010565	yes	yes
O_2+	31.98983	yes	yes
Ar+	39.962383	yes	yes
CO_2+	43.98983	yes	yes
$C_8H_5O_3$+	149.02386	yes, added	no
W182+	181.94821	no, removed	yes
W184+	183.95093	yes	yes
W186+	185.95436	no, removed	yes
$C_5H_{15}O_3Si_3$+	207.0329	yes, added	no

S3.2. Air beam

The airbeam correction was applied using the average of all runs within the experiment's duration. The correction factor for changes in the air beam was typically in the range 0.98–1.0.

S3.3. Background subtraction

The background subtraction algorithm was applied to the entire experiment uniformly using the default Tofwerk parameterization with Width = 15, Noise scaling = 1.0, f2 = 0.05, N = 20, and including a low-pass filter.

S3.4. Peak shape factor

In order to prepare the data for quantification, a peak shape and peak shape factor are chosen based on a common ion averaged over the entire dataset. The shape factor, v, corrects the fitted peak area for shape irregularities, and is equal to the ratio of the integral of the average peak to that of a perfect Gaussian (Corbin et al., 2015; Sueper et al., 2011). The shape factor was found for each experiment using PIKA 1.25C with the ions Ar+ and O_2+ (for lefthand side of the pseudo-Gaussian), and O_2+ (for the righthand side of the pseudo-Gaussian). The final v was 1.0774 in this case.

S3.5. Preparation for high-resolution fitting

The background-subtracted, airbeam-corrected data for the open, closed and difference mass spectra series (Pedro Compuzano-Jost, personal communication), with a resolution of ~50k ToF bins min^{-1}, were exported as plain text. The mass calibration parameters ($p_1(t)$, $p_2(t)$, and $p_3(t)$ from Eqn. S1.1) were also exported with 1-min resolution.

The data are imported into MATLAB R2021a. For each run, the x_{ToF} bins are converted to x_{mass} values ranging from about m/z = 10 to 400 by rearranging Eqn. S1.1:

$$x_{mass} = \left(\frac{x_{ToF} - p_1(t)}{p_2(t)}\right)^{1/p_3(t)} \quad \text{Eq. S2}$$

As before, the Open and Closed spectra have different fitting parameters. The Diff mass spectra are assigned to the Open calibration parameters.

S3.6. Fitting a Gaussian curve to peaks in the high-resolution mass spectrum

Following Corbin et al. (2015), a superposition of up to four Gaussian curves is fit to the peaks found within each unit mass. MATLAB was used to fit these. The i^{th} curve is described by

$$G_i(x_{mass}) = h_i \exp\left(\frac{-\left(x_{mass} - (\mu_i^0 + \delta\mu)\right)^2}{w^2}\right) \quad \text{Eq. S3}$$

where $G(x_{mass})$ is the value in Hz/ns observed by the multichannel plate, x_{mass} is the m/z axis, h_i is the height of the i^{th} peak, μ_i is the m/z value of the i^{th} peak, and w is the Gaussian width parameter (Corbin et al. 2015 and Sueper et al. 2011‡). For each unit mass, $2i + 2$ parameters are generally fit, e.g., for three peaks the fitted parameter matrix will consist of h_1, h_2, h_3, $\delta\mu$, and w for each unit mass of interest, with 1-min resolution. The peaks are allowed to shift together by $\delta\mu$ = m/z ±0.0015 to help correct for variability in the mass calibration. Fitting is performed for masses of interest separately. For example, to find the ion flux at m/z 35, only the ToF data between m/z 34.8 to m/z 35.2 are fit.

The mass accuracy of our measurements was estimated for the salt ions by comparing the fitted mass centroid to the nominal mass. Table S5 shows that our measurement captured the true mass of the salt ions within +200/-50 ppm.

The area of peak i is given by (Corbin et al. 2015)

$$A_i(x; v, h_i, \mu, w) = v h_i \int \exp\left(\frac{-\left(x - (\mu_i^0 + \delta\mu)\right)^2}{w^2}\right) dx \quad \text{Eq. S4}$$

Using the common integral definition [2,3],

$$\int e^{ax^2}\, dx = \sqrt{\pi/a},$$

and assigning $x' = x - (\mu_i^0 + \delta\mu)$ and $a = 1/w^2$, the indefinite integral of this work becomes $\int x^{ax'^2}\, dx = \sqrt{\pi/a} = w\sqrt{\pi}$, and the area of the i^{th} pseudo-Gaussian curve is then:

$$A_i(v, h_i, w) = v h_i w \sqrt{\pi} \qquad \text{Eq. S5}$$

The width w has units of m/z (w_{mass}), but the width in bins (w_{ToF}) is needed in Eq. S5. This is found by defining $x_{mass}^{hi\ or\ lo} = (\mu_i + \delta\mu) \pm w_{mass}/2$, then converting units as before: $x_{ToF}^{hi\ or\ lo} = p_1 + p_2 \left(x_{mass}^{hi\ or\ lo}\right)\text{^}p_3$, and then the width in bins is $w_{ToF} = x_{ToF}^{hi} - x_{ToF}^{lo}$. The calculated A is the ion flux, in units of Hz, and is referred to hereafter as I.

S3.7. Ions of interest

The chloride family consisted of m/z 35, 36, 37, 38, 58. The ions associated with PSL were 104, 103, and 78. These are three of the ions found in the NIST spectrum and in Hasager et al.[4]

S3.8. Particle Time-of-Flight Measurement

Particle Time-of-Flight measurements were performed using the unit-mass resolution data. A simple matrix deconvolution was performed with the default baseline region of 0.25. Conversion of the time of flight to particle velocity is accomplished via v_p = distance/time (m s^{-1}), where the distance of the PToF region is 0.295 m, and the resolution of 254 PToF bins (between 0.5 and 6 ms). Vacuum aerodynamic diameter (D_va) was found via:

$$D_\mathrm{va} = D_x \left(\frac{v_\mathrm{gas} - v_\mathrm{lens}}{v_\mathrm{p} - v_\mathrm{lens}} - 1\right)^{1/b} \qquad \text{Eq. S6}$$

where D_x = 20.443 nm, v_gas = 472.94 m s^{-1} is the velocity of the gas after acceleration in the aerodynamic lens, v_lens = 44.959 m s^{-1} is the gas velocity within the aerodynamic lens, D_x = 20.443 nm is a fitting constant, and b = 0.68347 is a fitting constant.

S3.9. Timeseries and signal-to-noise

The timeseries of two back-to-back HTDMA-AMS experiments on April 26, 2022 was analyzed to determine the best peaks for quantification of salt, polystyrene, and the ionization efficiencies of these for our setup (Figures S2 and S3). The signal to noise ratio (SNR) of the styrene peaks to the background is defined by

$$\mathrm{SNR} = 2H/h \qquad \text{Eq. S7}$$

where $H = \max(y_{pk}) - \mathrm{mean}(y_{bg})$ and $h = 2 \times \mathrm{std}(y_{bg})$, y is the y-axis value, pk denotes the range of values within the peak, and bg denotes the values outside the peak. Table S5 shows the SNR for two experiments on April 26, 2022. The high-resolution mz104 ion was the best indicator of styrene. Figures S2 and S3 show the signal-to-noise ratio for salts and styrene peaks, and Table S5 and S6 give the values.

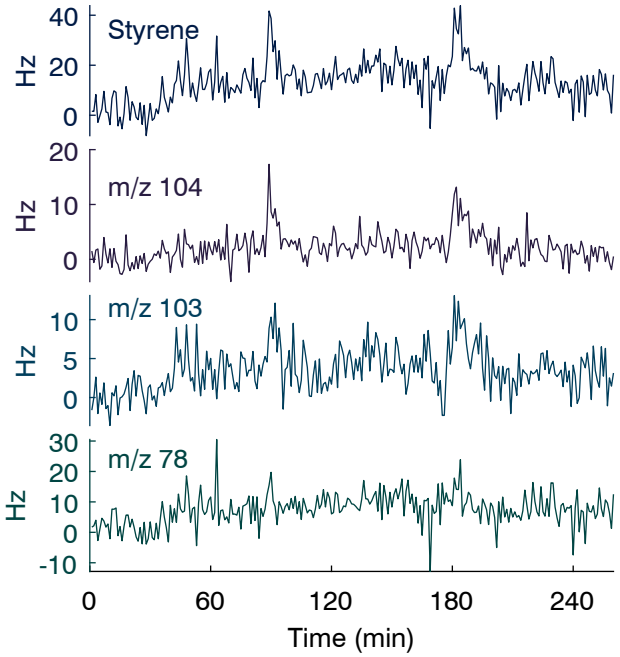

Figure S2. Timeseries of total styrene (m/z 104+103+78, family of ions) (top), m/z 104 (second), m/z 103 (third), and m/z 78 (bottom plot). Two experiments are shown, thus styrene detected at ~90 min and again at about 190 min. The experiment shown is from April 26, 2022. The second experiment started at 126 min.

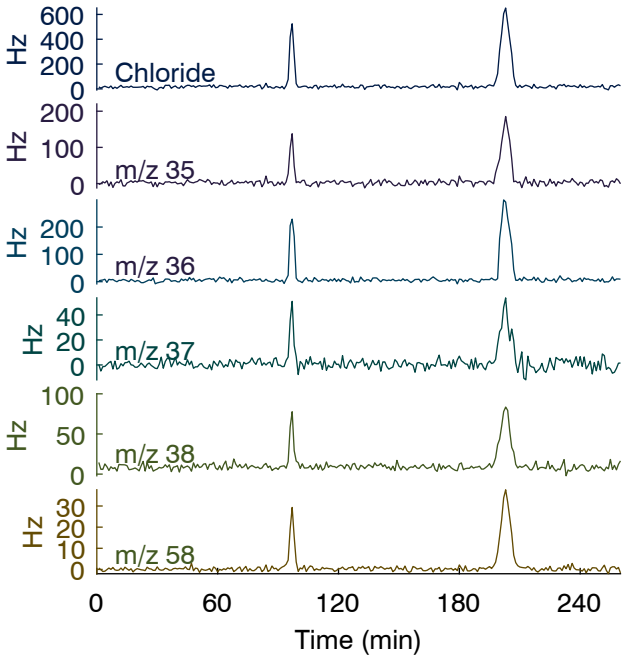

Figure S3. The second experiment started at 126 min. The scan duration was increased for the second experiment.

Table S5. Signal to noise ratios for April 26 dataset, experiments 1 and 2.

m/z	HR name	m/z nom	m/z fit	Signal-to-Noise, Figure S3	SQUIRREL[a]
35, 36, 37, 38, 58	Cl	n/a		48.9244, 37.4713	39.1505, 29.3009
Cl (default UMR)	n/a	n/a		n/a	39.1505, 29.3009
35	^{35}Cl	34.96885	34.9721, 34.9702	24.1901, 18.6686	30.2104, 21.0543
36	$H^{35}Cl$	35.97668	35.9787, 35.9756	34.9922, 24.6654	35.9901, 27.9141
37	^{37}Cl	36.9659	36.9704, 36.9705	19.3078, 13.8455	13.3420, 9.2272
38	$H^{37}Cl$	37.97373	37.9780, 37.9743	20.3368, 20.3368	12.8695, 10.1410
58	$Na^{35}Cl$	57.95862	57.9646, 57.9690	39.3738, 33.8367	13.0696, 9.8431

[a]ToF-AMS Analysis Toolkit 1.65C loaded with ToF_AMS_HRAnalysis_v1_25C.pxt.

Table S6. Signal to noise ratios for April 26 dataset, experiments 1 and 2.

Name	Signal-to-Noise, Figure S2	SQUIRREL[a]
mz104 + mz103 + mz78	4.5646, 4.9437	4.3998, 5.7753
mz104	8.3877, 6.0307	7.5514, 7.2198
mz103	2.7192, 3.9370	2.2459, 3.2193
mz78	2.3439, 3.2816	2.1227, 3.9865

[a]ToF-AMS Analysis Toolkit 1.65C loaded with ToF_AMS_HRAnalysis_v1_25C.pxt.

Section S4. Ionization Efficiency

The HSEMS scan on April 26, before the HTDMA-AMS scan, showed a peak in PSL and in salt (Figure 5 in the main text). The SEMS measurement gives 0.136 ug/m3 PSL and 33.12 μg/m^3 salts (density 1.2 g/cm^3 for salt, 1.05 for PSL).

Ionization efficiency (IE, ions per molecule) is obtained by the comparison of the condensation particle counter (CPC) measurement of molecules of species i per m^3 to the AMS measurement of ions of species i per m^3.

The relative ionization efficiency (RIE) is obtained by comparison to the nitrate ionization efficiency:

$$RIE_i = \frac{IE_i}{IE_{NO3}} \times \frac{M_{w,NO3}}{M_{w,i}} \qquad \text{Eq. S8}$$

S4.1. Nitrate

Table S7 shows the results of the nitrate calibration. Particles are assumed to be pure ammonium nitrate, and the sum of the signal at m/z 30 (NO^+, m/z 29.99799) and 46 (NO_2^+, m/z 45.9929) is used to quantify nitrate ionization efficiency. The molar masses of NO_3 and NH_4NO_3 are 62 (61.98782) and 80, respectively.

The volume concentration of particulate matter (PM) is found using the CPC measurement of number concentration and the mobility diameter (D):

$$c_{\mathrm{CPC}}\left(\frac{\mathrm{cm^3\ PM}}{\mathrm{m^3\ air}}\right) = \left(c_{\mathrm{CPC}}\frac{\#\ \mathrm{of\ particles}}{\mathrm{cm^3\ air}}\right)\left(\frac{\pi}{6}D^3\ \mathrm{nm^3}\right)\left(\frac{10^6\ \mathrm{cm^3\ air}}{\mathrm{m^3\ air}} \times \frac{10^{-21}\ \mathrm{cm^3\ PM}}{\mathrm{nm^3\ PM}}\right) \qquad \text{Eq. S9}$$

Volume concentration is converted to mass concentration (ammonium nitrate ρ = 1.72 g cm^{-3}):

$$c_{\mathrm{CPC}}\left(\frac{\mu\mathrm{g\ PM}}{\mathrm{m^3\ air}}\right) = \left(c_{\mathrm{CPC}}\ \frac{\mathrm{cm^3\ PM}}{\mathrm{m^3\ air}}\right)\left(\rho\ \frac{\mathrm{g\ PM}}{\mathrm{cm^3\ PM}}\right)\left(\frac{10^6\ \mu\mathrm{g}}{\mathrm{g}}\right) \qquad \text{Eq. S10}$$

The mass concentration of NO_3 is extracted from the whole:

$$c_{\mathrm{CPC}}\left(\frac{\mu\mathrm{g\ NO_3}}{\mathrm{m^3\ air}}\right) = c_{\mathrm{CPC}}\left(\frac{\mu\mathrm{g\ PM}}{\mathrm{m^3\ air}}\right) \times \frac{62\ \mu\mathrm{g\ NO_3}}{80\ \mu\mathrm{g\ PM}} \qquad \text{Eq. S11}$$

Thus, the calculation for 300 nm particles is:

$$c_{\mathrm{CPC}}\left(\frac{\mu\mathrm{g\ NO_3}}{\mathrm{m^3\ air}}\right) = c_{\mathrm{CPC}}(\mathrm{cm^{-3}}) \times \frac{\pi}{6}(300\ \mathrm{nm})^3 \times 10^{-9} \times 1.72 \times \frac{62}{80} \qquad \text{Eq. S12}$$

Mass concentration is then converted to a rate of molecules per second:

$$c_{\mathrm{CPC}}\left(\frac{\mathrm{molec\ NO_3}}{\mathrm{s}}\right) = c_{\mathrm{CPC}}\left(\frac{\mu\mathrm{g\ NO_3}}{\mathrm{m^3\ air}}\right)\left(\frac{10^{-6}\ \mathrm{g}}{\mu\mathrm{g}}\right)\left(\frac{1}{M_w}\frac{\mathrm{mol}}{\mathrm{g}}\right)\left(N_A\ \frac{\mathrm{molec}}{\mathrm{mol}}\right)\left(Q\ \frac{\mathrm{cm^3}}{\mathrm{s}}\right)\left(10^{-6}\ \frac{\mathrm{m^3}}{\mathrm{cm^3}}\right) \qquad \text{Eq. S13}$$

where N_A = 6.02214076e23 is Avogadro's number and Q is the flow rate into the AMS.

Table S7. Ammonium nitration ionization efficiency calibration.[a]

Measured, CPC $c_{\mathrm{CPC}}\left(\frac{\#\ \mathrm{of\ particles}}{\mathrm{cm^3\ air}}\right)$	Eq S3.2 $c_{\mathrm{CPC}}\left(\frac{\mu\mathrm{g\ PM}}{\mathrm{m^3\ air}}\right)$	Eq S3.5 $c_{\mathrm{CPC}}\left(\frac{\mathrm{molec\ NO_3}}{\mathrm{s}}\right)$	Measured, AMS mz30 + mz46 $\left(\frac{\mathrm{ions}}{\mathrm{s}}\right)$
812.0	15.30201295	1.65e11	25499.3
593.7	11.18818361	1.20e11	18873.0
366.0	6.897212733	7.43e10	11658.7
154.0	2.902105904	3.12e10	4607.13
16.2	0.3052864652	3.29e9	407.658
IE_{NO3} is 1.56077×10^{-7} with an R^2 of 0.999766			

[a] The ammonium nitrate calibration took place on Feb. 17, 2022. Q was 1.108 cm^3 s^{-1}.

A line is fit showing measured AMS signal as a function of molecules per second measured by the CPC. The slope of this line, 1.56077×10^{-7}, was taken to be IE_{NO3}, and the regression R^2 value was 0.999766.

S4.2. Chloride

Table S8 shows the results of the chloride calibration. In this case, experiments were averaged and one value each of c_{CPC} and c_{AMS} were used (rather than fitting a line, as with ammonium nitrate). The chloride ionization efficiency is quantified using the sum of the high-resolution ions, $^{35}Cl^+$, $H^{35}Cl^+$, $^{37}Cl^+$, $H^{37}Cl^+$, and $Na^{35}Cl^+$, corresponding to ions at m/z 35, 36, 37, 38, and 58.

Based on the HTDMA CPC signal, the concentration of particles passed to the AMS is c_{CPC} = 4.97 µg m^{-3} (averaged over two runs) of sea salt, assuming a density of 2.16 g cm^{-3} (Eq S3.1,2). This is not the inverted total concentration, but rather the raw count, which is subsequently re-routed to the AMS in the modified setup (Figure 1, path D-2). The HTDMA and AMS experiments were done sequentially with the same sample on the same day. The

mass ratio of Cl to all ions in the dry sea salt is 0.53628028, thus the mass concentration of Cl is 2.67 µg m^{-3}.

Mass concentration is converted to molecules per second via:

$$c_{\mathrm{CPC}}\left(\frac{\text{molec Cl}}{\text{s}}\right) = c_{\mathrm{CPC}}\left(\frac{\mu\text{g Cl}}{\text{m}^3}\right)\left(\frac{10^{-6}\text{ g}}{\mu\text{g}}\right)\left(\frac{1}{M_w}\frac{\text{mol}}{\text{g}}\right)\left(N_A\frac{\text{molec}}{\text{mol}}\right)\left(\frac{10^{-6}\text{ m}^3}{\text{cm}^3}\right)\left(Q\frac{\text{cm}^3}{\text{s}}\right) \quad \text{Eq. S14}$$

using the molar mass of Cl, M_w = 34.96885 g mol^{-1} and a flow rate Q = 1.6347292 cm^3 s^{-1}on April 26, 2022. The result is 7.5×10^{10} molecules per second. Applying a collection efficiency, CE, of 0.25 (typical of a dry salt aerosol) (Ovadnevaite et al.[5]), the value is reduced to CE × c_{CPC} = 1.9×10^{10} molecules per second. This value is directly compared to the average AMS signal (ions/s) to obtain the ionization efficiency:

$$\mathrm{IE_{Cl}} = \frac{(\mathrm{CE})\left(I\frac{\text{ions Cl}}{\text{s}}\right)}{\left(c_{\mathrm{CPC}}\frac{\text{molec Cl}}{\text{s}}\right)} \quad \text{Eq. S15}$$

Results are printed in Table S8 and in the main text. The relative ionization efficiency is obtained via:

$$\mathrm{RIE_{Cl}} = \frac{\mathrm{IE_{Cl}}}{\mathrm{IE_{NO_3}}}\frac{M_{w,\mathrm{NO_3}}}{M_{w,\mathrm{Cl}}} \quad \text{Eq. S16}$$

Table S8. Chloride ionization efficiency calibration using sea salt.[a]

m/z	35	36	37	38	58	SUM
m/z HR (g/mol)	34.96885	35.97668	36.9659	37.97373	57.95862	
Ion ID	^{35}Cl+	H^{35}Cl+	^{37}Cl+	H^{37}Cl+	Na^{35}Cl+	
c_{CPC} (µg PM m^{-3})						4.97
c_{CPC} (µg Cl m^{-3})						2.67
c_{CPC} (molec Cl s^{-1})						7.5035×10^{10}
Exp 1 (ions s^{-1}) [b]	137.701	228.907	50.8788	77.7011	29.3237	524.5116
Exp 2 (ions s^{-1})	185.389	299.257	53.6422	83.5137	37.673	659.4749
Average (ions s^{-1})					**AVG:**	591.9932
Collection Efficiency [c]						0.25
Ionization Efficiency of Cl (ion / molec)						3.1558×10^{-8}
RIE of Cl						0.3584

[a] The experiments took place on April 26, 2022. Q was 1.6347292 cm^3 s^{-1}. [b] Exp 1 and Exp 2 are two separate HTDMA scans on the same day. [c] Value for dry salt[5]

S4.3. Polystyrene

Table S9 shows the polystyrene ionization efficiency calculation, which followed a similar method as described for chloride. The collection efficiency of the salt-coated PSL was assumed to be 0.25, similar to chloride and appropriate for salts in the AMS.[5]

Table S9. Polystyrene ionization efficiency calibration.[a]

m/z	78	103	104	SUM
m/z HR (g/mol)	78.0514	103.0591	104.0649	
Ion ID			C_8H_8+	
c_{CPC} (μg PS m^{-3})				0.0233785
c_{CPC} (molec C_8H_8 s^{-1}) [b]				2.2116×10^{8}
Exp 1 (ions s^{-1}) [c]	23.8567	13.0868	13.1677	43.8104 [d]
Exp 2 (ions s^{-1})	19.7181	12.1157	17.3222	41.6820 [d]
Average (ions s^{-1})			**AVG:**	42.7462
Collection Efficiency				0.25
Ionization Efficiency of PS (ion / molec)				4.9669×10^{-8}
RIE of PS				0.1896

[a] The experiments took place on April 26, 2022. Q was 1.6347292 cm^3 s^{-1}. [b] After converting the observed mass into the equivalent concentration of styrene monomers. [c] Exp 1 and Exp 2 are two separate HTDMA scans on the same day. [d] Equal to the peak of the combined timeseries.

Section S5. Supplement to the Results

S5.1. Enhancement of Separation After Hygroscopic Growth

Figure S4 shows the size distribution (dN/dD, cm^{-3}) measured by the DMA 1 (Figure 1, route A, B-1) juxtaposed with the size distribution measured by DMA 2 (the HTDMA, Figure 1 route A, B, C, D-1; dN/dD, cm^{-3}). The comparison in panel A illustrates the detection of polystyrene latex spheres in the dry size distribution. The comparison in panel B illustrates that the polystyrene latex spheres are no longer detected in the dry size distribution, but maybe detected after humidified separation in the HTDMA.

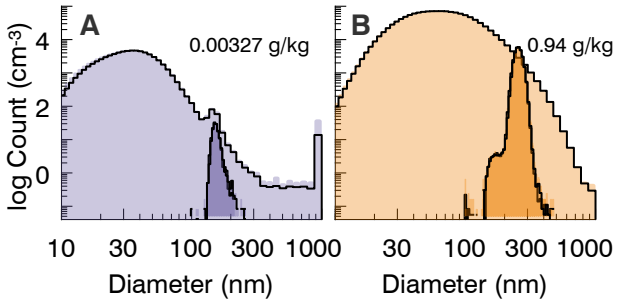

Figure S4. The entire particle distribution with the HTDMA-selected growth factors overlaid, showing the ability of the HTDMA to separate the salt and PSL peaks even at higher concentrations of total particles. Particles were generated by the atomizer. Panel A shows solution #2 (see Table 1), experiments #13, 14, 31, and 32 (see Table S1). Panel B shows solution #5, experiments #6, 7, 8, 25, and 26. Note that the size distributions are not inverted and have units of particles per cm^3.

S5.2. Growth Factors

Table S10 lists the hygroscopic growth factors displayed in the main text, Figure 5 and Figure 6. The table is broken into two figures to separate the atomizer from the ÆGOR experiments.

Table S10. Measured growth factors and the hygroscopicity of sea salt.

(A) Experiments using the atomizer

Salinity g kg^{-1}	GF 1 [a] -	GF 2 [b] -	a_w -	κ [c] -
NaN	NaN	NaN	74.9	
0	1.02	1.34	74.9	
0	1.00	NaN	74.9	
0.0001	1.02	NaN	74.9	
0.0005	1.02	NaN	74.9	
0.0033	1.04	1.33	74.9	
0.022	1.05	1.67	72.2	
0.14	1.08	1.72	74.4	1.40752
0.151	1.08	1.72	74.4	1.40752
0.239	1.09	1.72	74.4	1.40752
0.378	NaN	NaN	74.9	
0.596	1.16	1.72	74.4	1.40752
0.94	1.34	1.72	74.4	1.40752
6.21	1.70	NaN	74.9	
41	1.85	1.7	73.5	1.40799
		Avg:		1.408
		Std Dev:		1.48×10^{-4}

(B) Experiments using ÆGOR sea spray tank

Salinity g kg^{-1}	GF 1 -	GF 2 -	a_w -	κ -
0	1.01	1.25	74.9	
0	1.02	1.27	75.1	
0.01	NaN	NaN	74.7	
0.01	1.04	1.3	74.9	
0.0215	NaN	NaN	75.0	
0.0464	NaN	NaN	75.1	
0.0464	1.02	1.63	75.0	
0.1	NaN	NaN	74.9	
0.2154	1.07	1.73	74.8	1.40747
0.2154	1.07	1.77	76.35	1.40792
0.464	1.1	1.78	76.72	1.40789
0.464	1.12	1.77	76.35	1.40792
0.464	1.1	1.76	75.98	1.40737
1	1.14	1.77	76.35	1.40792
1	1.1	1.79	77.08	1.40807
1	1.13	1.77	76.35	1.40792
			Avg:	1.41
			Std Dev:	2.50×10^{-4}

[a] GF 1 is the growth factor of plastic. The dry diameter was 147 nm and dry size selection occurs at 150 nm for all experiments. [b] GF 2 is the growth factor of the salt mode. [c] κ is the hygroscopicity parameter of the salt (based on GF 2). Values are reported for salinity > 0.1 g kg^{-1}, where the contribution from plastics can be ignored. $\kappa = (GF^3 - 1)(1 - a_w)/a_w$.

References

‡ D. Sueper and collaborators, ToF-AMS Data Analysis Software Webpage, http://cires1.colorado.edu/jimenez-group/wiki/ index.php/ToF-AMS_Analysis_Software.

Corbin, C., A. Othman, J. D. Allan, D. R. Worsnop, J. D. Haskins, B. Sierau, U. Lohmann and A. A. Mensah, Peak-fitting and integration imprecision in the Aerodyne aerosol mass spectrometer: effects of mass accuracy on location-constrained fits, Atmos. Meas. Tech., 2015, 8, 4615–4636.

Hasager, F., Þ. N. Björgvinsdóttir, S. F. Vinter, A. Christofili, E. R. Kjærgaard, S. S. Petters, M. Bilde and M. Glasius, Development and validation of an analytical pyrolysis method for detection of airborne polystyrene nanoparticles.

Nicholas, C. P. and R. C. Yates, The Probability Integral, The American Mathematical Monthly, 1950, 57, 412–413.

Ovadnevaite, J,. D. Ceburnis, M. Canagaratna, H. Berresheim, J. Bialek, G. Martucci, D. R. Worsnop and C. O'Dowd, On the effect of wind speed on submicron sea salt mass concentrations and source fluxes, Journal of Geophysical Research: Atmospheres, DOI:10.1029/2011JD017379.

Petters, M. D.: Revisiting matrix-based inversion of scanning mobility particle sizer (SMPS) and humidified tandem differential mobility analyzer (HTDMA) data, Atmos. Meas. Tech., 14, 7909–7928, https://doi.org/10.5194/amt-14-7909-2021, 2021.

Weisstein,E. W., Gaussian Integral. From MathWorld--A Wolfram Web Resource. https://mathworld.wolfram.com/GaussianIntegral.html. Accessed January 2023.

Williams, Leah, 2010, What is My Vaporizer Temperature?, https://cires1.colorado.edu/jimenez-group/UsrMtgs/UsersMtg11/WilliamsAMSUsersMtg_2010_VapT.pdf. Hyytiala, Finland, 2010. Accessed January 2023.